β6 Integrin Subunit Deficiency Alleviates Lung Injury in a Mouse Model of Bronchopulmonary Dysplasia

Anna Hogmalm[1], Dean Sheppard[2], Urpo Lappalainen[1], and Kristina Bry[1]

[1]Department of Pediatrics, University of Gothenburg, Gothenburg, Sweden; and [2]Department of Medicine, Lung Biology Center, University of California San Francisco, San Francisco, California

Pulmonary inflammation is associated with the development of bronchopulmonary dysplasia in premature infants. We have previously shown that perinatal pulmonary expression of human IL-1β is sufficient to cause a lung disease similar to bronchopulmonary dysplasia, characterized by inflammation, impaired alveolarization, poor postnatal growth, and increased mortality in infant mice. The αvβ6 integrin plays a critical role in regulating inflammation in the adult lung. To study the role of the β6 integrin subunit in neonatal inflammatory lung disease, we compared the pulmonary development in IL-1β–expressing infant mice with wild-type or null β6 integrin loci. Absence of the β6 integrin subunit decreased the mortality and improved the postnatal growth of IL-1β–expressing pups. The disrupted alveolar development of IL-1β–expressing mice was improved by β6 integrin deficiency. IL-1β–expressing β6$^{-/-}$ pups had shorter alveolar chord length and thinner alveolar walls than IL-1β–expressing β6$^{+/+}$ pups. In addition, the absence of the β6 integrin subunit reduced IL-1β–induced neutrophil and macrophage infiltration into the alveolar spaces. β6 integrin subunit deficiency suppressed inflammation and goblet cell hyperplasia in the airways and alleviated airway remodeling in IL-1β–expressing mice. The expression of the chemoattractant proteins, keratinocyte-derived chemokine, macrophage-inflammatory protein–2, calgranulin A, and calgranulin B, of osteopontin, and of the chitinase-like lectins, Ym1 and Ym2, was lower in IL-1β–expressing β6$^{-/-}$ than in IL-1β–expressing β6$^{+/+}$ mice. We conclude that absence of the β6 integrin subunit protects the infant murine lung against IL-1β–induced inflammation and injury.

Keywords: IL-1; chemokine; inflammation; lung development; chronic lung disease

Bronchopulmonary dysplasia (BPD) is the major chronic lung disease in infants and children. The incidence of BPD, defined as the need for supplemental oxygen at 36 weeks postmenstrual age, is approximately 25% in infants weighing less than 1,500 g at birth (1, 2). This illness is an important cause of recurrent respiratory morbidity, poor growth, prolonged hospitalization, and increased mortality in infants. Lung pathology in BPD is characterized by inflammation, lack of alveolar septation, large alveoli, and impaired vascular development (3).

Inflammation is strongly associated with the development of BPD. Maternal chorioamnionitis, a common antecedent of premature birth (4), increases the newborn's risk of developing BPD

CLINICAL RELEVANCE

The pathogenetic mechanisms causing bronchopulmonary dysplasia, the most important inflammatory lung disease in infants, are largely unknown. The present study demonstrates that absence of the β6 integrin subunit, an activator of transforming growth factor-β, protects the neonatal murine lung against a bronchopulmonary dysplasia–like illness. These findings improve our understanding of the pathogenetic mechanisms of inflammatory lung injury in the neonate.

(5). Treatment of premature infants with mechanical ventilation and oxygen promotes lung inflammation and the development of BPD (1, 6–8). Neutrophils and macrophages accumulate early after birth, and persist in the lungs of infants who develop BPD (9). The levels of several inflammatory and chemotactic factors are increased in the lungs of infants developing BPD (10–14).

IL-1β, a central cytokine involved in the initiation and persistence of inflammation (15), is increased in amniotic fluid in chorioamnionitis and preterm labor (16). Elevated amniotic fluid concentration of IL-1β is associated with development of BPD (17). Levels of IL-1β are also increased postnatally in tracheal aspirates of premature infants who subsequently develop BPD (10, 11). Through the use of a transgenic mouse model, in which human IL-1β (hIL-1β) is expressed in the lung epithelium in an inducible manner, we have previously shown that perinatal expression of IL-1β causes a lung disease clinically and histologically similar to BPD (18). Alveolarization, which, in the normal murine lung, occurs from Postnatal Day (PN) 5 to PN28 (19), is disrupted by IL-1β. IL-1β–expressing infant mice have pulmonary infiltration with neutrophils and macrophages, lack of alveolar septation, abnormal vascular development, poor postnatal growth, and increased mortality (18).

Integrins are cell-surface proteins that regulate cell growth, migration, and survival. The αvβ6 integrin is a transmembrane glycoprotein that is expressed predominantly in epithelial cells (20, 21), and acts as a receptor for the extracellular matrix proteins, fibronectin, tenascin and vitronectin. The β6 integrin subunit pairs exclusively with the αv subunit, and its expression is markedly upregulated in epithelial cells in multiple organs, including the lung, in response to inflammation and injury (21). Adult mice deficient in the β6 integrin subunit develop spontaneous inflammation (22, 23) and age-dependent emphysema (24), but are protected from bleomycin-induced pulmonary fibrosis (25) and edema (26), implying that this integrin plays important roles in acute and chronic lung diseases. Blocking the αvβ6 integrin has recently been shown to alleviate IL-1β–induced acute lung injury in adult mice (27). The αvβ6 integrin is an *in vivo* activator of the profibrotic cytokine, transforming growth factor (TGF)–β1 (25), which causes abnormal lung development and fibrosis in newborn mice (28). The involvement of the β6 integrin subunit in neonatal inflammatory lung injury has not previously been investigated.

The aim of this study was to examine the role of the β6 integrin subunit in IL-1β–induced pulmonary disease in infant mice. The present results demonstrate that absence of the β6 integrin subunit decreases lung inflammation, improves lung alveolar development, and enhances postnatal growth and survival in IL-1β–expressing infant mice.

MATERIALS AND METHODS

Transgenic Mice

Double-transgenic rat Clara cell secretory protein (rCCSP)–reverse tetracycline transactivator (rtTA)–(tetracycline operator [tetO])₇ CMV-hIL-1β mice, which express the hIL-1β transgene in the presence of doxycycline, were generated as previously described (29). Mice bearing the rtTA transgene driven by the rCCSP promoter were mated with mice bearing the mature hIL-1β transgene driven by a tetracycline-responsive promoter ((tetO)$_7$CMV), to produce bitransgenic rCCSP–rtTA–(tetO)$_7$CMV–hIL-1β and single-transgenic rCCSP–rtTA pups. To specifically study the effects of hIL-1β, single-transgenic rCCSP–rtTA littermates were used as control animals (30).

To investigate the role of the β6 integrin subunit in IL-1β–induced lung injury, mice deficient in the β6 integrin subunit were mated with transgenic rCCSP–rtTA mice and transgenic (tetO)$_7$CMV–hIL-1β mice. The single-transgenic offspring were then mated to produce bitransgenic rCCSP–rtTA–(tetO)$_7$CMV–hIL-1β and single-transgenic rCCSP–rtTA β6$^{-/-}$ mice. All the mice were in an FVB/N background.

The mice were genotyped by PCR analysis of tail DNA using primers specific for transgene constructs as previously described (29). For genotyping of the β6 integrin gene, the following primers were used: forward, 5′-TAG CTT CCA GCC AAG GTG GG-3′; and reverse, 5′-TCT GAG GGA CTG GTA TGT GTG TCC-3′.

For clarity, the following abbreviations are used: control/β6$^{+/+}$ mouse, rCCSP–rtTA mouse with wild-type β6 integrin loci; control/β6$^{-/-}$ mouse, rCCSP–rtTA mouse with null β6 integrin loci; IL-1β/β6$^{+/+}$ mouse, rCCSP–rtTA–(tetO)$_7$CMV–hIL-1β mouse with wild-type β6 integrin loci; IL-1β/β6$^{-/-}$ mouse, rCCSP–rtTA–(tetO)$_7$CMV–hIL-1β mouse with null β6 integrin loci.

Animal Care

The mice were housed in pathogen-free conditions, and all experiments were conducted in accordance with ethics committee guidelines at the University of Gothenburg. All animals were given access to water and chow *ad libitum*. For sample collection of fetal lungs on Embryonic Day (E) 14, fetuses were removed by hysterotomy after anesthesia with intraperitoneal injection of a mixture of ketamine, xylazine, and acepromazine to the pregnant dam. For lung sample collection from infant mice on PN0 and PN7, pups were anesthetized by intraperitoneal injection of a mixture of ketamine, xylazine, and acepromazine, the abdomen was opened, and the animal was exsanguinated by transection of the abdominal aorta. The day of plug was counted as E0, and the day of birth was counted as PN0.

Administration of Doxycycline

To induce hIL-1β transgene expression in the lungs of bitransgenic pups, doxycycline (0.5 mg/ml; Sigma, St. Louis, MO) was administered in drinking water to pregnant and nursing dams from the beginning of pregnancy until pups were killed on PN0 or PN7. The doxycycline solution was changed three times per week and protected from light by covering cage bottles with aluminum foil.

Lung Histology and Immunohistochemistry of Inflammatory Cells

Lungs on PN0 and PN7 were inflation-fixed by instillation of 4% PBS-buffered paraformaldehyde fixative at a pressure of 25 cm H$_2$O, as previously described (29). After overnight fixation at +4°C, the tissue was processed through conventional paraffin embedding. Tissue sections (5 μm) were stained with hematoxylin and eosin or Alcian blue/periodic acid Schiff (PAS), with Mayer's hematoxylin as counterstain. The numbers of PAS-positive and PAS-negative cells were counted within the airways, and the percentage of PAS-positive cells per airway

was calculated. The following antibodies were used for immunohistochemistry: monoclonal rat anti-mouse neutrophil (clone 7/4; Serotec, Oxford, UK); monoclonal rat anti-mouse Mac3 (clone M3/84; BD Pharmingen, San Diego, CA); and biotinylated rabbit anti-rat secondary antibody (Vector Laboratories, Burlingame, CA). Avidin–biotin peroxidase (Vectastain Elite ABC; Vector Laboratories) and NovaRED (Vector Laboratories) were used according to the manufacturer's instructions. Sections immunostained for neutrophils and macrophages were counterstained with Mayer's hematoxylin. Immunostained neutrophils and macrophages in the airspaces and distal septal walls were counted in at least 10 nonoverlapping, high-power fields (HPFs) (400× magnification) from 5–6 animals per group. In addition, the areas of airspaces and septa were measured, and the average numbers of positive cells per square millimeter were calculated for each of these areas.

Analysis of Airspace Size and Alveolar Wall Thickness

Measurement of distal airspace size at PN7 was performed from lung sections stained with hematoxylin and eosin, with the mean chord length as a measure of alveolar size. A minimum of 10 representative, nonoverlapping fields from lungs of 6 mice of each genotype were analyzed. Areas of bronchiolar airways and blood vessels were excluded from the analysis. Chord length analysis was performed using the public domain program, NIH Image, with a chord length macro (available from the National Institutes of Health at http://rsb.info.nih.gov/nih-image), as previously described (29).

The same images at PN7 were used for measuring the thickness of the alveolar walls. A minimum of 10 representative, nonoverlapping fields from lungs of 6 mice of each genotype were analyzed by drawing over 40 straight lines in each field across the narrowest segment of the alveolar wall. The mean length of lines crossing the alveolar walls was determined with the NIH Image software.

Detection of Apoptotic Cells with Terminal Transferase dUTP Nick-End Labeling

In situ terminal transferase dUTP nick-end labeling for the detection of apoptotic or dying cells was performed as previously described on PN0 and PN7 (31). A distinct color reaction within the cells was regarded as representing DNA fragmentation. Terminal transferase dUTP nick-end labeling–positive cells in the airspaces and septal walls were counted in at least 10 nonoverlapping HPFs (400× magnification) from four to six animals per group. In addition, the areas of airspaces and septa were measured, and the average numbers of positive cells per square millimeter were calculated separately in the areas of airspace and septa.

Proliferation

Cell proliferation was studied by immunohistochemical detection of the proliferation marker, Ki-67 (32). Polyclonal rabbit anti-human antibody that cross-reacts with murine Ki-67 (Novocastra Laboratories Ltd., Newcastle Upon Tyne, UK) and biotinylated goat anti-rabbit secondary antibody (Vector Laboratories) were used. Avidin–biotin peroxidase (Vectastain Elite ABC; Vector Laboratories) and 3.3′-diaminobenzidine (Vector Laboratories) were used according to the manufacturer's instructions. Sections were counterstained with nuclear fast red. The total number of Ki-67–positive cells in the distal lung was counted in at least 10 nonoverlapping fields (400× magnification) from 5 animals per group.

Inflammation on E14

To study the presence of inflammation in fetal mice, lungs from β6$^{+/+}$ and β6$^{-/-}$ mice that had not received doxycycline were collected on E14 for histological evaluation and mRNA analysis. The chests of fetal mice were opened, and the lungs were fixed in 4% PBS-buffered paraformaldehyde for histology. After overnight fixation at +4°C, the tissue was processed through conventional paraffin embedding. Tissue sections (5 μm) were stained with hematoxylin and eosin, and immunostained for macrophages and neutrophils. The numbers of positive cells were counted in at least 5 HPFs.

Quantitative RT-PCR

Total RNA was isolated using TRIzol reagent (Invitrogen, Carlsbad, CA), according to the manufacturer's instructions, and treated with

RNase-free DNase (DNA-free; Ambion, Austin, TX). Total RNA (1 μg) was reverse transcribed (Omniscript; Qiagen, Hilden, Germany), and 20 ng of cDNA was analyzed by quantitative real-time PCR, as previously described (18). Primer sequences (forward and reverse, respectively, 5′–3′) used were as follows: β-actin, TCC GTA AAG ACC TCT ATG CCA ACA, CTC AGG AGG AGC AAT GAT CTT GAT; CXC chemokine receptor (CXCR)2, CCT CAG ACT TTT GGC TTC CTC GT, CGC AGT GTG AAC CCG TAG CAG A; keratinocyte-derived chemokine (KC; CXCL1), AAA CCG AAG TCA TAG CCA CAC TCA, CTT GGG GAC ACC TTT TAG CAT CTT; macrophage inflammatory protein (MIP)–2 (CXCL2), CCC CCT GGT TCA GAA AAT CAT C, AAC TCT CAG ACA GCG AGG CAC ATC; monocyte chemoattractant protein (MCP)–1 (CCL2), GCT CTC TCT TCC TCC ACC ACC AT, GCT CTC CAG CCT ACT CAT TGG GAT; MCP-3 (CCL7), TCT GCC ACG CTT CTG TGC CT, GCT CTT GAG ATT CCT CTT GGG GAT; osteopontin, CGG TGA AAG TGA CTG ATT CTG GCA, CGC AAG GAG ATT CTG CTT CTG AGA; calgranulin A (S100A8; myeloid-related protein 8), GAG CAA CCT CAT TGA TGT CTA, TGC ATT GTC ACT ATT GAT GTC CA; calgranulin B (S100A9; myeloid-related protein 14), GCC AAC AAA GCA CCT TCT CAG AT, GCC ATC AGC ATC ATA CAC TCC TCA A; serum amyloid A3 (SAA3), TGC TCG GGG GAA CTA TGA TGC T, CCA CTC GTT GGC AAA CTG GTC A; (tetO)$_7$CMV-hIL-1β, CCA TCC ACG CTG TTT TGA CCT C, ACC AAG CTT TTT GCT GTG AGT CC; Ym1 (chitinase 3–like 3), GCT CAT TGT GGG ATT CCA GCA, CCT CAG TGG CTC CTT CAT CAA AA; Ym2 (chitinase 3-like 4), TTG GAG GAT GGA AGT TTG GAC CT, TGA CGG TTC TGA GGA GTA GAG ACC A. The results were normalized to β-actin mRNA levels.

Cytokine Measurement in Lung Homogenates

Lung tissue (PN7) was homogenized in PBS containing a protease inhibitor (Complete protease inhibitor; Roche Diagnostics, Basel, Switzerland). The homogenized tissue was centrifuged to remove cell debris, and the supernatant was used for analysis. Concentration of hIL-1β in lung homogenate was measured with DuoSet hIL-1β ELISA development kit (R&D Systems, Abingdon, UK), specific for hIL-1β, with no cross-reactivity with murine IL-1β. DuoSet ELISA development kits were used to quantify mouse KC, MIP-2, MCP-1, and osteopontin, as well as active TGF-β1 in whole-lung homogenates at PN7. Acidification of the samples was used according to the manufacturer's instructions to transform latent TGF-β1 to the immunoreactive form, to enable measurement of total TGF-β1. After the acid activation, the samples were neutralized before ELISA, according to the manufacturer's instructions. Assay standard concentration ranges were 3.9–250 pg/ml (hIL-1β, MCP-1), 7.8–1,000 pg/ml (active TGF-β1), and 15.6–1,000 pg/ml (KC, MIP-2, osteopontin). Total protein concentration was measured by the bicinchoninic acid method, according to the manufacturer's instructions (Sigma).

Statistical Analysis

Measurement values are presented as means (±SEM). Groups of normally distributed data were compared by t test with GraphPad Prism software (GraphPad Software Inc., San Diego, CA). Postnatal survival data were analyzed by Kaplan-Meier survival analysis and log-rank test. P values less than 0.05 were considered statistically significant.

RESULTS

Expression of hIL-1β in the Lungs of Infant Bitransgenic Mice

To verify that the absence of the β6 integrin subunit did not change the levels of hIL-1β in the lungs of bitransgenic pups, doxycycline was administered to pregnant and lactating dams from plug date until the pups were killed at PN7. The levels of mature hIL-1β mRNA and protein were similar in IL-1β/β6$^{+/+}$ and IL-1β/β6$^{-/-}$ pups (hIL-1β/β-actin mRNA, IL-1β/β6$^{+/+}$ 0.57 ± 0.34 [n = 7]; IL-1β/β6$^{-/-}$, 0.61 ± 0.29 [n = 12], P = 0.8; hIL-1β protein/total protein, IL-1β/β6$^{+/+}$ 67 ± 29 ng/mg [n = 9]; IL-1β/β6$^{-/-}$ 59 ± 11 ng/mg [n = 7], P = 0.4).

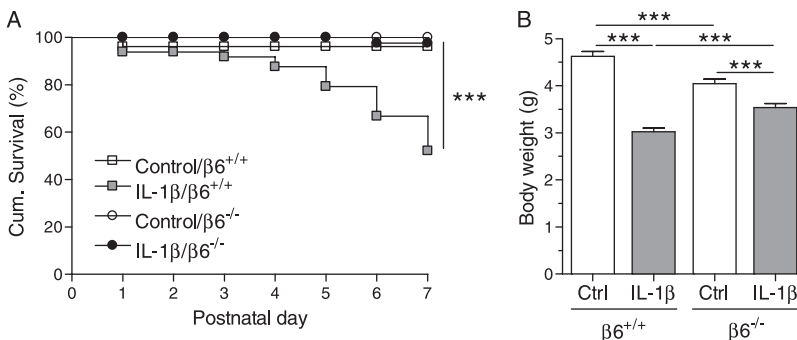### Absence of the β6 Integrin Subunit Improved the Survival of IL-1β–Expressing Mice

All control/β6$^{-/-}$ mice survived until PN7, whereas two control/β6$^{+/+}$ pups died at or soon after birth (Figure 1A). Approximately 50% of the IL-1β/β6$^{+/+}$ mice died by 7 days of age (Figure 1A, data from Bry and colleagues [18]). In contrast, only 2% (one pup) of the IL-1β/β6$^{-/-}$ mice died by 7 days of age (Figure 1A).

Absence of the β6 Integrin Subunit Improved Postnatal Growth in IL-1β–Expressing Mice

The birth weights of control/β6$^{+/+}$, control/β6$^{-/-}$, IL-1β/β6$^{+/+}$, and IL-1β/β6$^{-/-}$ pups were similar (data not shown). IL-1β/β6$^{+/+}$ and IL-1β/β6$^{-/-}$ mice weighed less than their littermate controls at PN7 (Figure 1B). Although control/β6$^{-/-}$ mice weighed less than control/β6$^{+/+}$ mice, IL-1β/β6$^{-/-}$ mice weighed more than IL-1β/β6$^{+/+}$ mice (Figure 1B).

Absence of the β6 Integrin Subunit Improved Alveolar Septation and Alveolar Wall Thinning in IL-1β–Expressing Mice

To examine whether the absence of the β6 integrin subunit affected alveolar development in infant mice expressing IL-1β, the alveolar chord length and alveolar wall thickness were studied in infant IL-1β–expressing and control mice with wild-type or null β6 loci. In control/β6$^{+/+}$ and control/β6$^{-/-}$ pups, alveolar septation was underway at PN7, as expected, whereas alveolarization was disrupted in both IL-1β/β6$^{+/+}$ and IL-1β/β6$^{-/-}$ mice (Figures 2A–2E). On histological sections, the size of the distal airspaces appeared smaller in IL-1β/β6$^{-/-}$ than in IL-1β/β6$^{+/+}$ mice (Figures 2B and 2D). This result was confirmed by alveolar chord length measurement that revealed shorter alveolar chord length in IL-1β/β6$^{-/-}$ mice than in IL-1β/β6$^{+/+}$ mice (Figure 2E).

Figure 1. The absence of the β6 integrin subunit improved the survival and postnatal growth of IL-1β–expressing mice. Doxycycline was administered to the dams from the beginning of pregnancy until the pups were killed at Postnatal Day (PN) 7. (*A*) Postnatal survival until PN7. IL-1β decreased the survival rate of β6$^{+/+}$ pups (log-rank test, P < 0.0001 IL-1β/β6$^{+/+}$ versus all other groups), but not of β6$^{-/-}$ pups (P = 0.3 IL-1β/β6$^{-/-}$ versus control/β6$^{-/-}$). All control/β6$^{-/-}$ pups survived until PN7, whereas two control/β6$^{+/+}$ pups died at or soon after birth (P = 0.2 control/β6$^{+/+}$ versus control/β6$^{-/-}$). The total numbers of animals studied were: control/β6$^{+/+}$, 47; control/β6$^{-/-}$, 41; IL-1β/β6$^{+/+}$, 48; IL-1β/β6$^{-/-}$, 42. (*B*) Body weights at PN7. IL-1β/β6$^{-/-}$ pups weighed more than IL-1β/β6$^{+/+}$ pups, although control/β6$^{-/-}$ pups weighed less than control/β6$^{+/+}$ pups. Data are presented as means (±SEM) (n = 20–34 per group). ***P < 0.001.

In the absence of doxycycline administration, alveolar chord length was similar in control/β6$^{+/+}$, control/β6$^{-/-}$, IL-1β/β6$^{+/+}$, and IL-1β/β6$^{-/-}$ mice (control/β6$^{+/+}$, 35.0 ± 2.38 μm [n = 4]; control/β6$^{-/-}$, 37.3 ± 1.42 μm [n = 5]; IL-1β/β6$^{+/+}$, 37.5 ± 2.63 μm [n = 4]; IL-1β/β6$^{-/-}$, 37.0 ± 0.97 μm [n = 5]).

Because alveolar wall thinning is an important part of normal lung development (33), we measured alveolar wall thickness in the mice at PN7. The alveolar wall thickness was similar in control/β6$^{+/+}$ and control/β6$^{-/-}$ mice (Figure 2F). IL-1β expression prevented alveolar septal thinning in both β6$^{+/+}$ and β6$^{-/-}$ mice (Figure 2F). However, the alveolar walls were thinner in IL-1β/β6$^{-/-}$ than in IL-1β/β6$^{+/+}$ mice (Figure 2F).

Absence of the β6 Integrin Subunit Suppressed IL-1β–Induced Neutrophil and Macrophage Infiltration into the Lung

Although the number of neutrophils within the alveolar septa was similar in control/β6$^{-/-}$ and control/β6$^{+/+}$ pups, control/β6$^{-/-}$ pups had more neutrophils in the alveolar spaces than control/β6$^{+/+}$ pups (Figures 3A and 3B). Although IL-1β caused infiltration of neutrophils into the lung in both β6$^{+/+}$ and β6$^{-/-}$ mice, absence of the β6 integrin subunit suppressed the IL-1β–induced neutrophil migration into the alveolar spaces (Figure 3A). No difference was found in the number of alveolar septal neutrophils between IL-1β/β6$^{-/-}$ and IL-1β/β6$^{+/+}$ mice (Figure 3B). Thus, the distribution of neutrophils between alveolar septa

and lumen was different in β6$^{-/-}$ and β6$^{+/+}$ mice. In IL-1β/β6$^{+/+}$ mice, 69% of the neutrophils in the alveolar region of the lung were in the alveolar spaces, whereas, in IL-1β/β6$^{-/-}$ mice, only 39% of the neutrophils were intra-alveolar (Figure 3C).

Most of the macrophages in the distal lung were in the alveolar lumen in all animals (Figure 3F). The numbers of macrophages in the alveolar lumen and alveolar septa were similar in control/β6$^{+/+}$ and control/β6$^{-/-}$ mice (Figures 3D and 3E). IL-1β increased the number of macrophages in both the alveolar lumen and alveolar septa in β6$^{+/+}$ mice, but only in the alveolar lumen in β6$^{-/-}$ mice (Figures 3D and 3E). Absence of the β6 integrin subunit suppressed IL-1β–induced macrophage infiltration into both the alveolar lumen and the septa (Figures 3D and 3E).

Absence of the β6 Integrin Subunit Suppressed the IL-1β–Induced Expression of Chemoattractants, of the Acute-Phase Protein SAA3, and of Osteopontin in the Lungs of Infant Mice

The higher number of neutrophils in the alveolar spaces in control/β6$^{-/-}$ mice compared with control/β6$^{+/+}$ mice was associated with increased mRNA and protein expression of the neutrophil-attractant CXC chemokines, KC and MIP-2, and mRNA expression of the CXC chemokine receptor, CXCR2, in the lungs of control/β6$^{-/-}$ mice compared with control/β6$^{+/+}$ mice (Figures 4A–4E). The mRNA expression of the monocyte
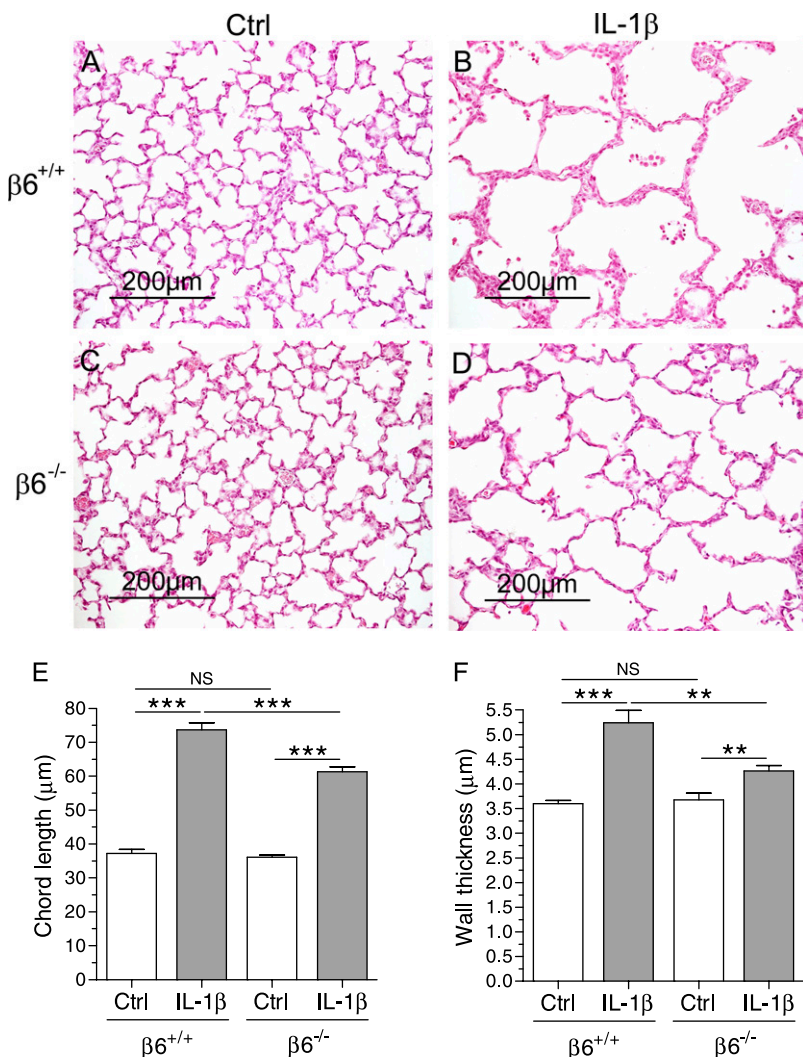

Figure 2. Alveolar septation and alveolar wall thinning in IL-1β–expressing mice was improved in mice deficient in β6 integrin subunit. Doxycycline was administered to the dams from the beginning of pregnancy until the pups were killed. (*A–D*) Lung histology at PN7. Normal alveolar septation is seen in control/β6$^{+/+}$ and control/β6$^{-/-}$ mice (*A* and *C*). Lack of septation in IL-1β/β6$^{+/+}$ appears less severe in IL-1β/β6$^{-/-}$ mice (*B* and *D*). *Scale bar*, 200 μm. (*E*) Mean alveolar chord length. IL-1β increased the chord length in both β6$^{+/+}$ and β6$^{-/-}$ mice compared with control animals. The chord length was shorter in IL-1β/β6$^{-/-}$ mice than in IL-1β/β6$^{+/+}$ mice. Data are presented as means (±SEM) (*n* = 6 per group). (*F*) Alveolar wall thickness. IL-1β–expressing mice had thicker alveolar walls than control mice at PN7. The alveolar walls were thinner in IL-1β/β6$^{-/-}$ mice than in IL-1β/β6$^{+/+}$ mice. Data are presented as means (±SEM) (*n* = 6 per group). **P < 0.01, ***P < 0.001. NS, not significant.
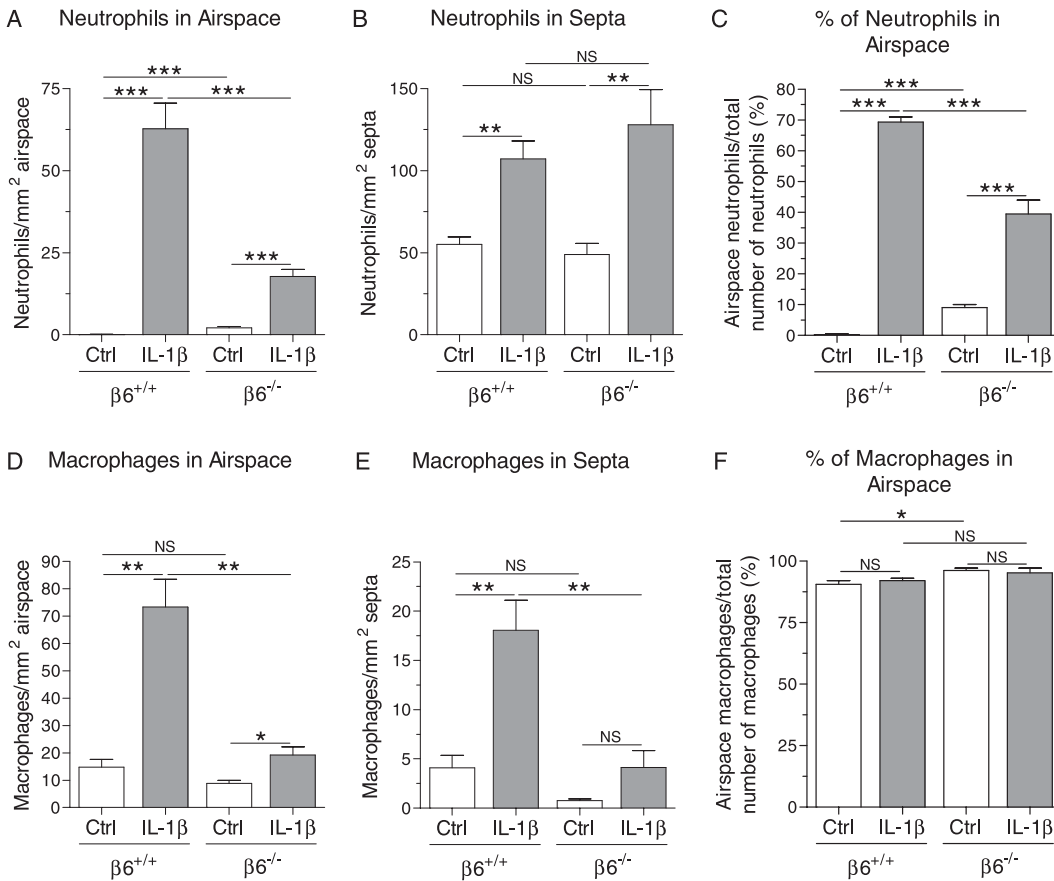
Figure 3. Neutrophils and macrophages in the lungs of infant mice. Dams received doxycycline from the beginning of pregnancy until the pups were killed at PN7. Neutrophils and macrophages were detected by immunohistochemistry and counted in the alveolar airspaces and alveolar septal walls in five to six animals per group. (*A*) The number of neutrophils in the alveolar airspaces was higher in IL-1β/β6$^{+/+}$ mice than in IL-1β/β6$^{-/-}$ mice. The number of cells is expressed per square millimeter of airspace area. (*B*) IL-1β increased the number of neutrophils in the alveolar septa in both β6$^{+/+}$ and β6$^{-/-}$ mice. The number of cells is expressed per square millimeter of alveolar septal area. (*C*) The distribution of neutrophils between the alveolar lumen and the alveolar walls was different in IL-1β/β6$^{+/+}$ and IL-1β/β6$^{-/-}$ mice. Most of the neutrophils in IL-1β/β6$^{+/+}$ mice and IL-1β/β6$^{-/-}$ mice were in the alveolar lumen and alveolar walls, respectively. The IL-1β–induced infiltration of macrophages to the alveolar spaces (*D*) and alveolar walls (*E*) was decreased in β6$^{-/-}$ mice. The number of macrophages is expressed per square millimeter of distal airspace (*D*) and septal area (*E*). (*F*) The majority of macrophages was found in the alveolar spaces in all groups of mice. Data are presented as means (±SEM). *$P < 0.05$, **$P < 0.01$, ***$P < 0.001$.

chemokines, MCP-1 and MCP-3, and the protein levels of MCP-1, were also higher in control/β6$^{-/-}$ than in control/β6$^{+/+}$ mice (Figures 4F–4H). Similarly, the mRNA expression of the chemotactic and proinflammatory proteins, S100A8, S100A9, and SAA3, was up-regulated in control mice in the absence of the β6 integrin (Figures 5A–5C). In contrast, absence of the β6 integrin subunit suppressed the mRNA expression and protein production of osteopontin in control mice (Figures 5D and 5E).

Although IL-1β increased the expression and production of the neutrophil chemokines, KC and MIP-2, in both β6$^{+/+}$ and β6$^{-/-}$ mice, the levels of these chemokines were lower in IL-1β/β6$^{-/-}$ mice than in IL-1β/β6$^{+/+}$ mice (Figures 4A–4D). Absence of the β6 integrin subunit also suppressed the IL-1β–induced mRNA expression of S100A8, S100A9, and SAA3, and the mRNA expression and protein production of osteopontin (Figures 5A–5E). In contrast, absence of the β6 integrin potentiated the IL-1β–induced expression of the monocyte chemoattractants, MCP-1 and MCP-3, and the production of MCP-1 in the lungs of infant mice (Figures 4F–4H). IL-1β increased CXCR2 mRNA expression similarly in β6$^{-/-}$ and β6$^{+/+}$ mice (Figure 4E).

Absence of the β6 Integrin Subunit Prevented Airway Remodeling and Suppressed the Expression of the Chitinase-Like Lectins, Ym1 and Ym2, in IL-1β–Expressing Mice

The airways of control/β6$^{+/+}$ and control/β6$^{-/-}$ mice were structurally normal (Figures 6A, 6C, and 6E). Expression of IL-1β caused thickening and goblet cell hyperplasia of the airway

epithelium and induced accumulation of inflammatory cells in the airways in mice with wild-type β6 loci (Figures 6B and 6E). Large numbers of lymphocytes were seen around the airways in IL-1β/β6$^{+/+}$ mice (Figure 6B). Absence of the β6 integrin subunit suppressed these pathological changes in the airways of IL-1β–expressing mice (Figures 6D and 6E). A majority of the airways in IL-1β/β6$^{+/+}$ had more than 80% goblet cells, whereas a majority of the airways in IL-1β/β6$^{-/-}$ had less than 20% goblet cells.

Because the chitinase-like lectins, Ym1 and Ym2, are up-regulated in airway inflammation (34, 35), we studied their expression in the lungs of infant mice. The mRNA expression of Ym1 and Ym2 was lower in control/β6$^{-/-}$ than in control/β6$^{+/+}$ mice (Figures 6F and 6G). The expression of both Ym1 and Ym2 was increased roughly 50-fold in IL-1β/β6$^{+/+}$ mice compared with control/β6$^{+/+}$ mice (Figures 6F and 6G). Although the expression of these chitinases was increased by IL-1β in mice lacking the β6 integrin subunit, the expression of Ym1 and Ym2 was much lower in IL-1β/β6$^{-/-}$ mice than in IL-1β/β6$^{+/+}$ mice (Figures 6F and 6G).

Apoptosis and Proliferation in the Lungs of Control and IL-1β–Expressing Mice

Dysregulated apoptosis and/or proliferation may contribute to the structural alterations in BPD (36–38). In addition, the numbers of inflammatory cells in the lungs could be affected by apoptosis. For these reasons, we studied apoptosis and proliferation in the lungs of newborn mice at PN0 and PN7. As previously described, a peak of apoptosis was seen in the lungs of control/β6$^{+/+}$ mice directly after birth (39) (Figures 7A–7C).
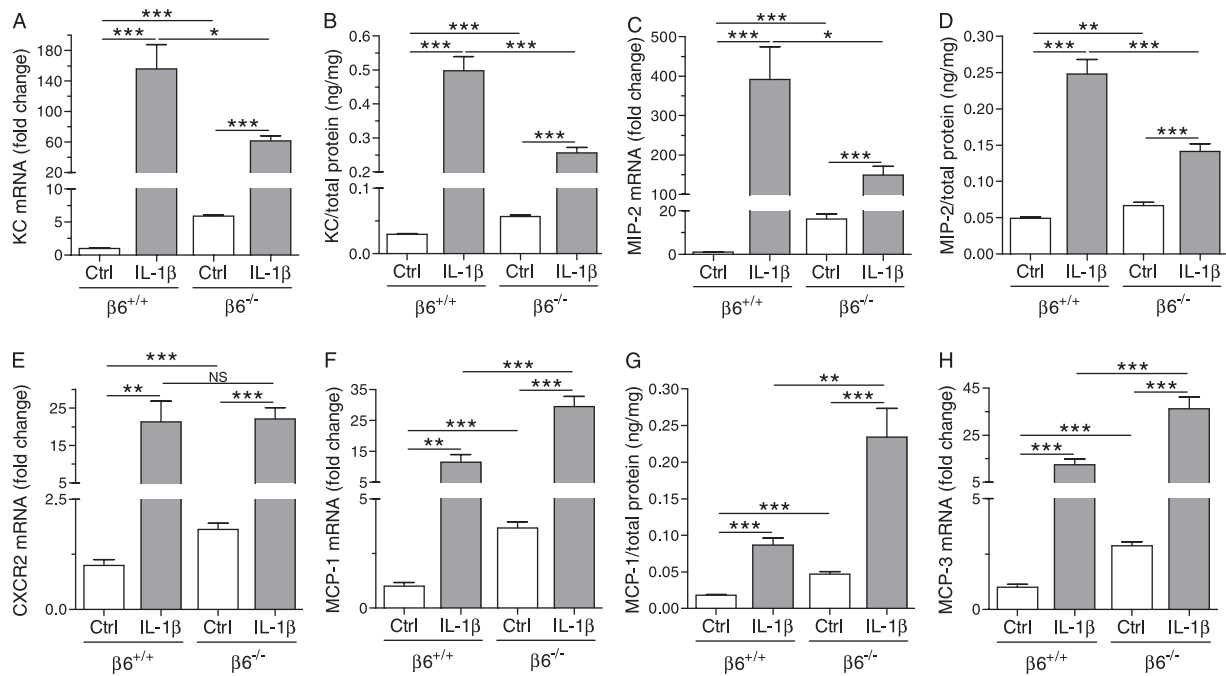
Figure 4. mRNA expression and protein levels of CC and CXC chemokines. Dams were given doxycycline throughout pregnancy and postnatally until the pups were killed at PN7. The IL-1β–induced mRNA expression and protein production of the CXC chemokines, keratinocyte-derived chemokine (KC) (*A* and *B*) and macrophage inflammatory protein (MIP)–2 (*C* and *D*), were decreased in β6$^{-/-}$ mice. IL-1β increased CXCR2 mRNA expression (*E*) similarly in β6$^{+/+}$ and β6$^{-/-}$ mice. Absence of the β6 integrin subunit increased the mRNA expression and protein production of monocyte chemoattractant protein (MCP)–1 (*F* and *G*), and the mRNA expression of MCP-3 (*H*), in both control mice and IL-1β–expressing mice. The mRNA expression levels are shown relative to the mRNA expression level of control/β6$^{+/+}$ mice, which was set to 1.0. Data are presented as means (±SEM) (*n* = 7–12 per group). *$P < 0.05$, **$P < 0.01$, ***$P < 0.001$.

Interestingly, apoptosis in the lungs at PN0 was suppressed by IL-1β in β6$^{+/+}$, but not in β6$^{-/-}$ mice (Figures 7A–7C).

As expected (39), apoptosis in control lungs decreased from PN0 to PN7 (Figures 7A–7C). IL-1β enhanced apoptosis in the lungs of both β6$^{+/+}$ and β6$^{-/-}$ mice at PN7 (Figure 7A). In addition, the lungs of control/β6$^{-/-}$ mice had more apoptosis than control/β6$^{+/+}$ mice at PN7 (Figure 7A). At PN7, IL-1β increased the numbers of apoptotic cells in the airspace in both β6$^{+/+}$ and β6$^{-/-}$ mice (Figure 7C). However, there was no difference in apoptosis between IL-1β/β6$^{+/+}$ and IL-1β/β6$^{-/-}$ mice in the airspaces (Figure 7C). Thus, differences in apoptosis did not explain the differences in the numbers of inflammatory cells in the alveolar spaces between IL-1β/β6$^{+/+}$ and IL-1β/β6$^{-/-}$ mice. Absence of the β6 integrin increased the number of apoptotic cells within the alveolar septa in both control and IL-1β–expressing mice at PN7 (Figure 7B). This suggests that increased apoptosis in the septa of IL-1β/β6$^{-/-}$ mice may have contributed to the septal thinning in these mice.

The number of proliferating cells, as studied by Ki-67 labeling, rose sharply from PN0 to PN7 in control/β6$^{+/+}$ lungs (Figure 7D). This is consistent with previous results showing a large increase in cell proliferation in the lung after birth (39). The total number of proliferating cells within the distal lung of control/β6$^{+/+}$ mice was approximately 30%, similar to results previously obtained in wild-type murine lungs at PN7 (40). No significant differences were seen in the numbers of proliferating cells between the four different genotypes at either PN0 or PN7 (Figure 7D).

Lack of Spontaneous Inflammation in Fetal β6 Integrin–Deficient Mice

β6 integrin deficiency leads to spontaneous inflammation in adult mice (22). Similarly, more neutrophils and higher expression of

inflammatory proteins were present in the lungs of the infant control/β6$^{-/-}$ mice than in control/β6$^{+/+}$ mice at PN7 (Figures 3A, 4A–4H, and 5A–5C). Because spontaneous inflammation in β6 integrin–deficient mice might protect their lungs against subsequent inflammation, we studied whether lack of β6 integrin caused inflammation in fetal mice at E14, the time at which hIL-1β production is first initiated by doxycycline administration (18). In this experiment, no doxycycline was given to pregnant mice, and the lungs of fetuses were harvested at E14. Importantly, there were no differences at this time point between β6$^{+/+}$ and β6$^{-/-}$ in the numbers of macrophages or neutrophils (Table 1). Furthermore, we found no difference in the mRNA expression of the following inflammatory genes in the lungs of β6$^{+/+}$ and β6$^{-/-}$ mice: KC, MIP-2, MCP-3, osteopontin, S100A8, S100A9, SAA3, Ym1, and Ym2 (Table 1). The expression of MCP-1 was higher in β6$^{+/+}$ than in β6$^{-/-}$ mice (1.44 ± 0.05 versus 1.19 ± 0.07; $P <$ 0.01) (Table 1). Thus, we found no evidence of enhanced inflammation in β6$^{-/-}$ fetuses compared with β6$^{+/+}$ fetuses at E14. The suppression of IL-1β–induced inflammation in β6 integrin–deficient infant mice is therefore unlikely due to a previous inflammation in the mice.

Active TGF-β1 in the Lungs of IL-1β–Expressing and Control Infant Mice

Because the αvβ6 integrin is an *in vivo* activator of TGF-β1, we measured the levels of active and total TGF-β1 in IL-1β/β6$^{+/+}$ and IL-1β/β6$^{-/-}$ mice and their controls at PN7. IL-1β increased the levels of active TGF-β1 in both β6$^{+/+}$ and β6$^{-/-}$ mice (Figure 8A). IL-1β–expressing mice deficient in β6 integrin tended to have lower levels of active TGF-β1, but the difference was not statistically significant (Figure 8A). The levels of total TGF-β1 did not significantly differ between the different genotypes (Figure 8B).
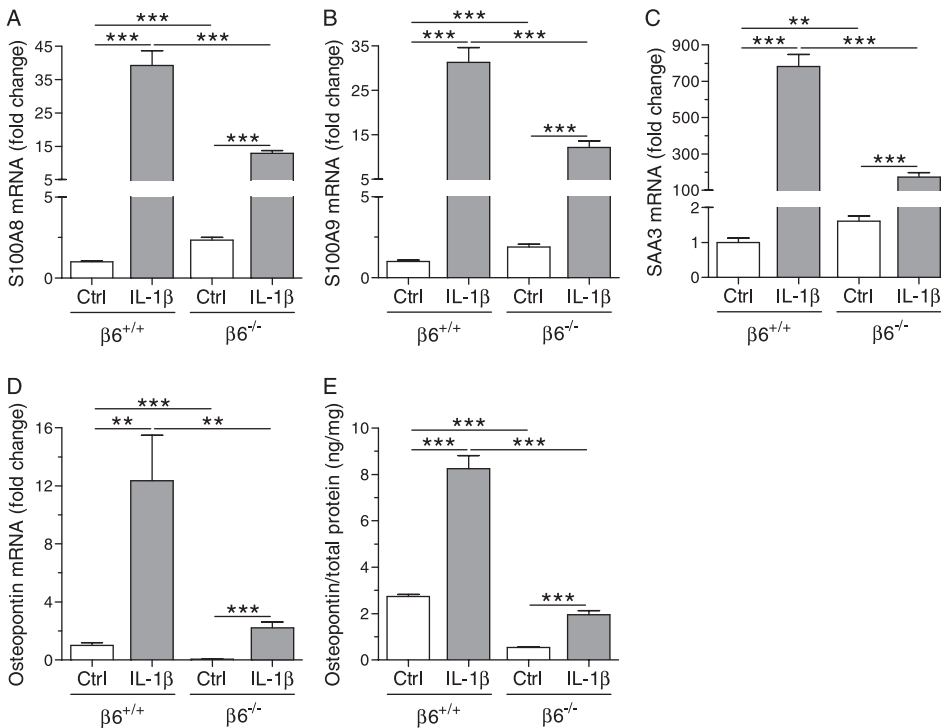
Figure 5. mRNA expression and protein production of inflammatory mediators in the lungs of infant mice. Dams were given doxycycline from beginning of pregnancy until the pups were killed at PN7. The IL-1β–induced expression of calgranulin A (S100A8) (*A*), calgranulin B (S100A9) (*B*), and serum amyloid A3 (SAA3) (*C*) was decreased in β6$^{-/-}$ mice. Absence of the β6 integrin subunit decreased the expression and production of osteopontin (*D* and *E*) in both control and IL-1β–expressing mice. The mRNA expression levels are shown relative to the mRNA expression level of control/β6$^{+/+}$ mice, which was set to 1.0. Data are presented as means (±SEM) (*n* = 8–11 per group). **$P < 0.01$, ***$P < 0.001$.

DISCUSSION

IL-1β–Induced Lung Disease in β6 Integrin–Deficient Mice

The present results demonstrate, for the first time, that absence of the β6 integrin subunit alleviates IL-1β–induced inflammation and injury in the lungs of infant mice. IL-1β–expressing mice deficient in the β6 integrin had lower mortality, improved growth, less pulmonary inflammation, less mucus metaplasia and remodeling in the airways, and better postnatal alveolar development than IL-1β–expressing mice with wild-type β6 loci.

Lung histology in infants with BPD is characterized by large distal airspaces and paucity of alveolar septation (3). While perinatal expression of hIL-1β disrupted alveolar septation in infant mice (18), the lungs of IL-1β/β6$^{-/-}$ mice had shorter alveolar chord length than those of IL-1β/β6$^{+/+}$ mice, indicating better septation in the absence of the β6 integrin subunit. Alveolar wall thinning occurring during alveolar development in the mammalian lung is thought to be important for normal gas exchange (33). In infants with BPD, the alveolar walls remain thick and hypercellular (41). Postnatal thinning of distal airspace walls failed to occur in IL-1β/β6$^{+/+}$ mice, whereas absence of the β6 integrin subunit improved alveolar wall thinning in mice expressing IL-1β.

Modulation of IL-1β–Induced Pulmonary Inflammation by β6 Integrin Deficiency

In adult mice, absence of the β6 integrin subunit causes pulmonary inflammation characterized by increased numbers of phagocytes in the bronchoalveolar lavage fluid (23). We found more neutrophils in the alveolar spaces of infant β6$^{-/-}$ control mice than in β6$^{+/+}$ control animals. In addition, the expression of the CXC chemokines, KC and MIP-2, of the CXC chemokine receptor, CXCR2, and of the CC chemokines, MCP-1 and MCP-3, was increased in the lungs of control/β6$^{-/-}$ mice compared with control/β6$^{+/+}$ mice. As expected, IL-1β expression caused pulmonary inflammation with neutrophils and

macrophages in both β6$^{+/+}$ and β6$^{-/-}$ mice. The IL-1β–induced immigration of neutrophils into the alveolar airspaces was suppressed in the lungs of mice lacking the β6 integrin subunit. The production of KC and MIP-2, essential for maximal neutrophil immigration into the alveolar spaces (42, 43), was inhibited in the lungs of IL-1β/β6$^{-/-}$ mice compared with IL-1β/β6$^{+/+}$ mice. Absence of the β6 integrin subunit lessened the infiltration of macrophages into the alveolar septa as well as the immigration of these cells into the airspaces in IL-1β–expressing lungs. However, the expression of the monocyte and T lymphocyte chemoattractants, MCP-1 and MCP-3 was increased in the lungs of IL-1β/β6$^{-/-}$ mice compared with IL-1β/β6$^{+/+}$ mice. These results are similar to those reported in adult mice in response to intratracheal bleomycin, where MCP-1 levels were higher at baseline and after bleomycin treatment in the lungs of β6$^{-/-}$ mice than in β6$^{+/+}$ mice (44).

In addition to CXC chemokines, the expression of other chemotactic proteins, including SAA3 and the S100A8 and S100A9 calgranulins, although enhanced by the absence of the β6 integrin in control mice, was strongly suppressed in IL-1β/β6$^{-/-}$ mice compared with IL-1β/β6$^{+/+}$ mice. SAA3, a member of the serum amyloid A family, functions as a chemotactic agonist for neutrophils and macrophages (45). S100A8 and S100A9 are potently chemotactic for neutrophils and monocytes (46) and up-regulate the expression of several chemokines, including KC, MIP-2, and MCP-1, by endothelial cells (47). Blocking S100A8 and S100A9 strongly inhibits the migration of neutrophils and macrophages into the alveolar spaces during streptococcal pneumonia, suggesting that these proteins regulate the migration of phagocytes through epithelial cells into the airspaces (46). Thus, the suppression of the expression of these proteins in IL-1β/β6$^{-/-}$ mice may have contributed to the reduced immigration of macrophages and neutrophils into the alveolar lumen in these mice.

Osteopontin functions as a proinflammatory and profibrotic cytokine (48), and participates in the development of type 2 inflammatory disorders, including asthma (49). Osteopontin expression was inhibited by β6 integrin deficiency in both control and IL-1β–expressing mice. Because osteopontin is chemotactic
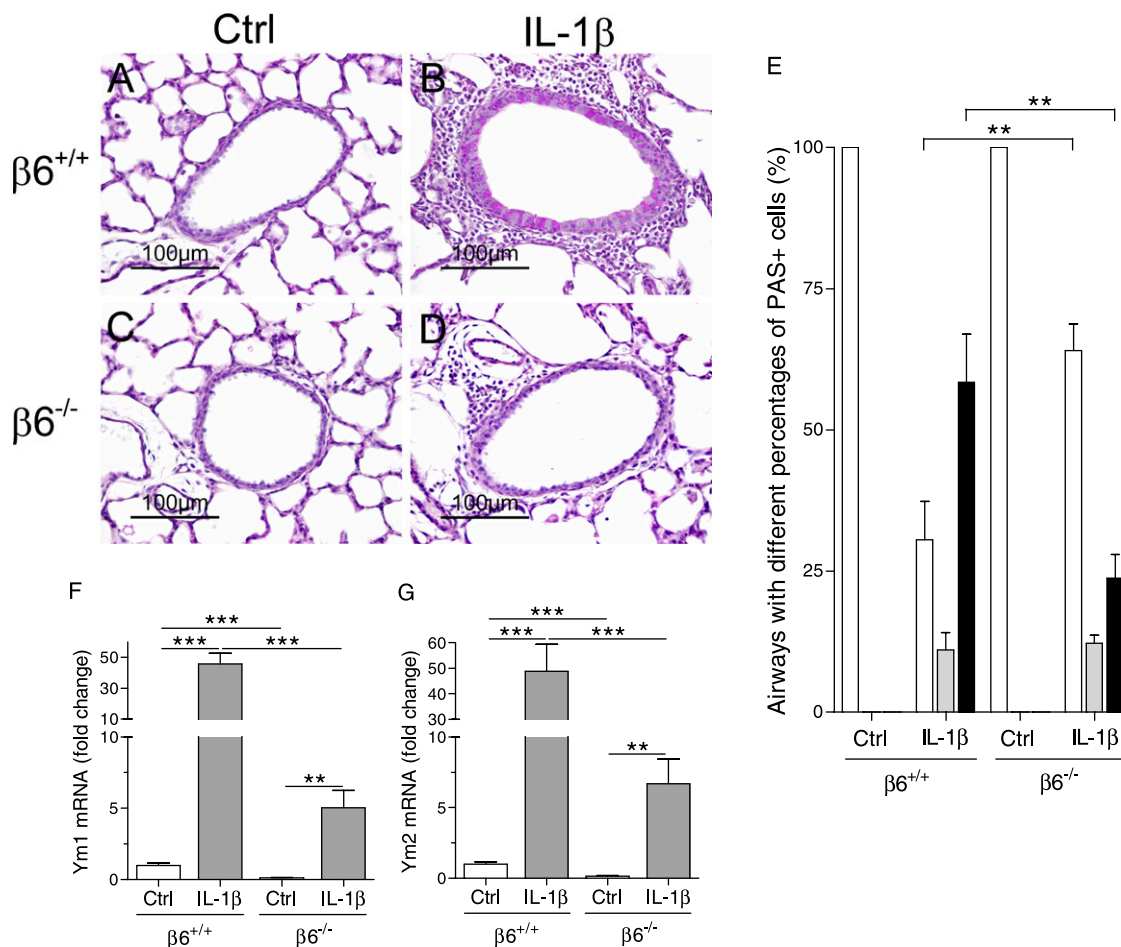
Figure 6. Airway structure and expression of the chitinases, Ym1 and Ym2. Dams were given doxycycline from the beginning of pregnancy until the pups were killed at PN7. (*A–D*) Airway histology, periodic acid Schiff (PAS) staining. The airways of control/β6$^{+/+}$ and control/β6$^{-/-}$ mice appear normal (*A* and *C*). Goblet cell hyperplasia, thickening of the airway epithelium, and accumulation of inflammatory cells are seen in the airways of IL-1β/β6$^{+/+}$ mice (*B*). In IL-1β/β6$^{-/-}$ mice, the airways were thinner, mucus production was sparse, and airway inflammation was suppressed (*D*). *Scale bars*, 100 μm. (*E*) Distribution (%) of airways with different percentages of PAS-positive cells. *Open bars*, airways having less than 20% goblet cells; *shaded bars*, airways having 20–80% goblet cells; *filled bars*, airways having more than 80% goblet cells. Absence of the β6 integrin decreased the IL-1β–induced goblet cell hyperplasia. β6 integrin deficiency reduced the expression of Ym1 (*F*) and Ym2 (*G*) in control and IL-1β–expressing mice. The mRNA expression levels are shown relative to the mRNA expression level of control/β6$^{+/+}$ mice, which was set to 1.0. Data are presented as means (±SEM) (*n* = 9–10 per group). **$P < 0.01$, ***$P < 0.001$.

for various cells, notably macrophages (50), decreased expression of osteopontin in IL-1β/β6$^{-/-}$ mice may have inhibited the influx of macrophages into the lungs of these mice.

Absence of the β6 integrin suppressed airway inflammation, goblet cell hyperplasia, and epithelial thickening induced by IL-1β in the lungs of infant mice. The expression of the chitinase-like lectins, Ym1 and Ym2, was strongly induced by IL-1β in mice with wild-type β6 integrin loci, whereas deficiency of β6 integrin subunit suppressed the expression of Ym1 and Ym2 in both control and IL-1β–expressing mice. Ym1 and Ym2 are up-regulated in allergic airway inflammation, and may play a role in the development of asthma (34, 35). Treatment with anti-sense Ym1 RNA reduces airway responsiveness in a model of allergic asthma (35).

Apoptosis and Proliferation in the Lungs

Apoptosis and proliferation play important roles in normal lung development. In the present study, the number of proliferating cells in the lungs rose sharply from PN0 to PN7, as expected (39), but no differences were found in cell proliferation between the

different genotypes at either time point. In rodents, there is a postnatal peak of apoptosis shortly after birth, a nadir in apoptosis around 1 week of age, and another peak appearing after the completion of alveolar septation at about 3 weeks of age (39). The postnatal peak of apoptosis appearing normally soon after birth was suppressed in IL-1β/β6$^{+/+}$, but not in IL-1β/β6$^{-/-}$ mice. Apoptosis was increased by IL-1β in both β6$^{+/+}$ and β6$^{-/-}$ mice at PN7. Dysregulated apoptosis may contribute to the structural aberrations associated with acute and chronic lung diseases, including BPD (36–38). On the other hand, enhanced apoptosis of mesenchymal cells has been associated with improved alveolarization and thinning of airspace walls (51). At PN7, apoptosis was enhanced in the alveolar septa of IL-1β/β6$^{-/-}$ mice compared with IL-1β/β6$^{+/+}$ mice. The combination of more apoptosis and less inflammation in the septal walls in IL-1β/β6$^{-/-}$ than in those of IL-1β/β6$^{+/+}$ mice may have contributed to the enhanced thinning of the septa in IL-1β/β6$^{-/-}$ mice compared with IL-1β/β6$^{+/+}$ mice. IL-1β enhanced the number of apoptotic cells within the airspaces in both β6$^{+/+}$ and β6$^{-/-}$ mice. Because the number of apoptotic cells within the alveolar lumen of IL-1β/β6$^{+/+}$ mice did not differ from those of IL-1β/β6$^{-/-}$ mice,
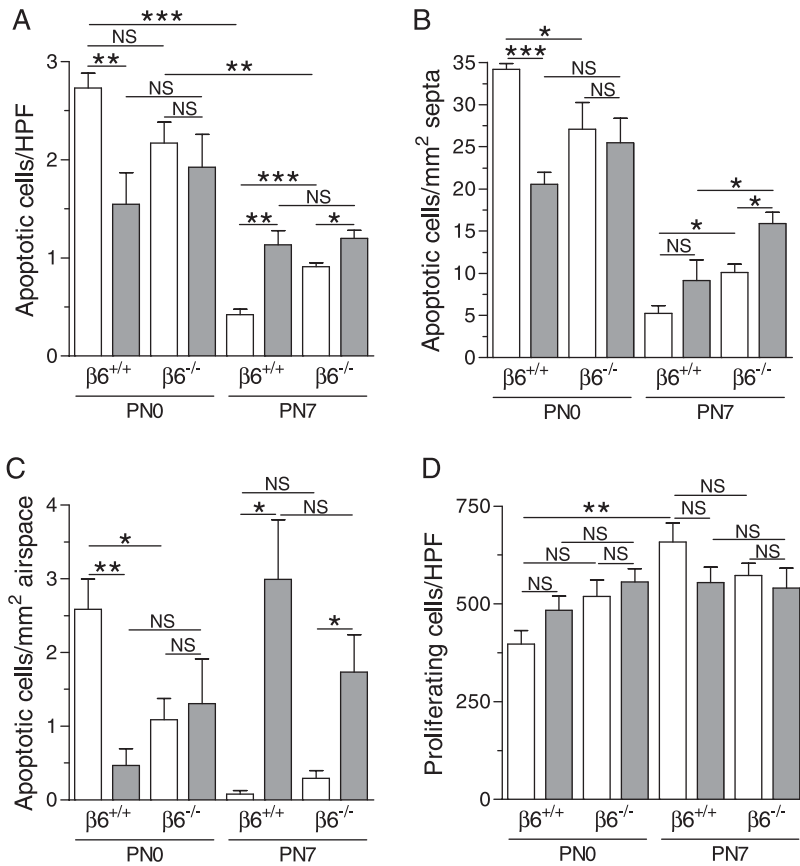
Figure 7. Apoptosis and proliferation in the distal lung. Dams were given doxycycline from the beginning of pregnancy until the pups were killed at PN0 or PN7. (*A*) Total number of distal terminal transferase dUTP nick-end labeling–positive cells (apoptotic cells) per high-power field (HPF). Apoptotic cells in the distal septa (*B*) and distal airspace (*C*) per square millimeter septal and airspace area, respectively. (*D*) Total number of Ki-67 (proliferation marker)–positive cells in the distal lung per HPF. *Open bars*, control mice; *shaded bars*, IL-1β–expressing mice. Data are presented as means (±SEM) (n = 4–6 per group). *$P < 0.05$, **$P < 0.01$, ***$P < 0.001$.

differences in apoptosis did not explain why fewer inflammatory cells were present in the alveolar spaces in IL-1β/β6$^{-/-}$ mice than in IL-1β/β6$^{+/+}$ mice.

Lack of Spontaneous Inflammation in β6 Integrin–Deficient Fetal Mice

Deficiency of β6 integrin causes spontaneous inflammation in adult mice (22, 23). Similarly, we observed higher numbers of neutrophils (but not of macrophages) in the alveolar spaces and higher levels of inflammatory proteins at PN7 in the lungs of control/β6$^{-/-}$ infant mice than in those of control/β6$^{+/+}$ mice. Because inflammation in β6 integrin–deficient mice before IL-1β expression might protect the mice against subsequent hIL-1β–induced inflammation, we studied inflammation and the expression of inflammatory genes in the lungs of fetal mice at E14, the time point at which hIL-1β production in bitransgenic mice becomes inducible by doxycycline administration (18). At E14, we could not detect increased inflammation or enhanced expression of inflammatory genes in β6 integrin–deficient fetuses compared with fetuses with wild-type β6 integrin loci. Thus, the suppression of hIL-1β–induced inflammation and lung injury in β6 integrin–deficient mice is probably not due to tolerance to inflammatory injury arising from a previous inflammation in the mice.

TGF-β1, β6 Integrin, and IL-1β–Induced Lung Injury

IL-1β increased the levels of active TGF-β1 in the lungs of β6$^{+/+}$ and β6$^{-/-}$ mice. The αvβ6 integrin is a known activator of latent TGF-β1 (25). Consistent with other studies (25, 52), we found no significant difference between the levels of active TGF-β1 in the lungs of IL-1β/β6$^{+/+}$ and IL-1β/β6$^{-/-}$ mice. The expression of β6 integrin, as well as that of hIL-1β in the present model, is restricted to epithelial cells in the lung (20, 21). αvβ6-

mediated TGF-β activation is thought to involve an induced conformational change in integrin-bound latent TGF-β complexes, without causing release of free TGF-β (25). Lack of the β6 integrin thus leads to a local deficiency in active TGF-β1 (25), which is difficult to detect in whole-tissue homogenates.

Overexpression of bioactive TGF-β1 in neonatal mouse lung has been shown to cause abnormal alveolar development in the newborn mouse (28). Mice with inducible dominant mutation of the TGF-β type II receptor are protected against impaired alveolarization induced by hypoxia (53). Moreover, administra-

TABLE 1. LACK OF SPONTANEOUS INFLAMMATION IN β6-DEFICIENT MICE AT EMBRYONIC DAY 14

	β6$^{+/+}$	β6$^{-/-}$
Macrophages/HPF	4.86 ± 0.42	4.14 ± 0.55
Neutrophils/HPF	0.64 ± 0.56	0.47 ± 0.18
KC mRNA	0.75 ± 0.22	0.70 ± 0.23
MIP-2 mRNA	0.23 ± 0.04	0.36 ± 0.06
MCP-1 mRNA	1.44 ± 0.05*	1.19 ± 0.07
MCP-3 mRNA	0.40 ± 0.02	0.36 ± 0.07
Osteopontin mRNA	0.15 ± 0.02	0.19 ± 0.03
S100A8 mRNA	0.15 ± 0.07	0.17 ± 0.04
S100A9 mRNA	0.10 ± 0.04	0.16 ± 0.03
SAA3 mRNA	0.16 ± 0.07	0.37 ± 0.20
Ym1 mRNA	0.24 ± 0.10	0.43 ± 0.13
Ym2 mRNA	0.35 ± 0.14	0.70 ± 0.20

Definition of abbreviations: HPF, high-power field; KC, keratinocyte-derived chemokine; MCP, monocyte chemoattractant protein; MIP, macrophage inflammatory protein; S100A8, calgranulin A; S100A9, calgranulin B; SAA3, serum amyloid A3.

mRNA expression of inflammatory genes (relative to β-actin) (n = 8–12). For macrophage and neutrophil counts, four to eight animals per group were studied. Data are shown as means (±SEM).

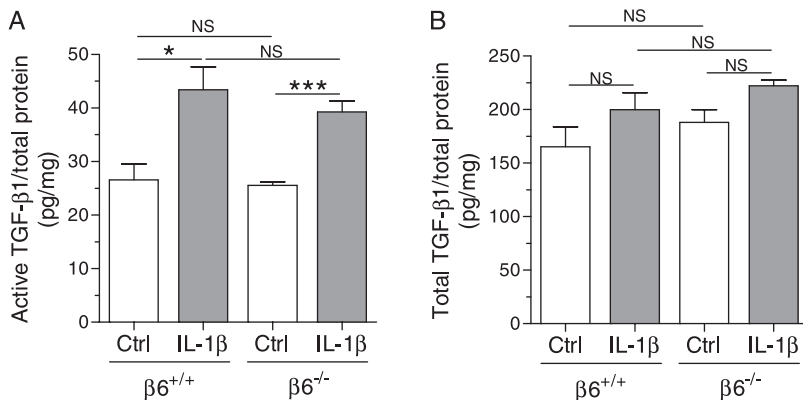* $P < 0.01$ versus β6-deficient mice. All other differences are not significant.

Figure 8. Active and total transforming growth factor (TGF)–β1 in the lungs of infant mice. Dams were given doxycycline from the beginning of pregnancy until the pups were killed at PN7. (*A*) The level of active TGF-β1 was increased in the lungs of IL-1β/β6$^{+/+}$ and IL-1β/β6$^{-/-}$ mice compared with control/β6$^{+/+}$ and control/β6$^{-/-}$ mice, respectively. (*B*) The level of total TGF-β1 did not significantly differ between the genotypes. The level of TGF-β1 was determined by ELISA in lung homogenates from 5–10 animals per group. Data are presented as means (±SEM). *$P < 0.05$, ***$P < 0.001$.

tion of TGF-β1–neutralizing antibodies was recently shown to improve alveolar development in newborn mice in which lung injury was induced by chronic hyperoxia (54).

Adult mice deficient in β6 integrin are protected from pulmonary fibrosis due to a local decrease in active TGF-β1 in the lung (25). In adult murine lungs, transient overexpression of IL-1β by adenoviral gene transfer increases lung vascular permeability (27). Inhibition of αvβ6 integrin and/or TGF-β reduced the IL-1β–induced increase in lung vascular permeability and the quantity of pulmonary edema (27). *In vitro* studies have shown that inhibition of the αvβ6 integrin and/or TGF-β signaling blocks the IL-1β–mediated protein permeability across alveolar epithelial monolayers (27). Together, these data support the idea that inhibition of TGF-β1 activity is a mechanism by which β6 deficiency protects the newborn lung against IL-1β–induced injury.

References

1. Jobe AH, Bancalari E. Bronchopulmonary dysplasia. *Am J Respir Crit Care Med* 2001;163:1723–1729.
2. Lemons JA, Bauer CR, Oh W, Korones SB, Papile L-A, Stoll BJ, Verter J, Temprosa M, Wright LL, Ehrenkranz RA, et al. Very low birth weight outcomes of the National Institute of Child Health and Human Development Neonatal Research Network, January 1995 through December 1996. *Pediatrics* 2001;107:e1.
3. Coalson JJ. Pathology of new bronchopulmonary dysplasia. *Semin Neonatol* 2003;8:73–81.
4. Goldenberg RL, Hauth JC, Andrews WW. Intrauterine infection and preterm delivery. *N Engl J Med* 2000;342:1500–1507.
5. Watterberg KL, Demers LM, Scott SM, Murphy S. Chorioamnionitis and early lung inflammation in infants in whom bronchopulmonary dysplasia develops. *Pediatrics* 1996;97:210–215.
6. Jobe AH, Kramer BW, Moses HL, Newnham JP, Ikegami M. Decreased indicators of lung injury with continuous positive expiratory pressure in preterm lambs. *Pediatr Res* 2002;52:387–392.
7. Yoder BA, Siler-Khodr T, Winter VT, Coalson JJ. High-frequency oscillatory ventilation: effects on lung function, mechanics, and airway cytokines in the immature baboon model for neonatal chronic lung disease. *Am J Respir Crit Care Med* 2000;162:1867–1876.
8. Deng HUI, Nicholas Mason S, Auten RL Jr. Lung Inflammation in hyperoxia can be prevented by antichemokine treatment in newborn rats. *Am J Respir Crit Care Med* 2000;162:2316–2323.
9. Merritt TA, Cochrane CG, Holcomb K, Bohl B, Hallman M, Strayer D, Edwards DK 3rd, Gluck L. Elastase and alpha 1-proteinase inhibitor activity in tracheal aspirates during respiratory distress syndrome: role of inflammation in the pathogenesis of bronchopulmonary dysplasia. *J Clin Invest* 1983;72:656–666.

10. Kakkera DK, Siddiq MM, Parton LA. Interleukin-1 balance in the lungs of preterm infants who develop bronchopulmonary dysplasia. *Biol Neonate* 2005;87:82–90.
11. Kotecha S, Wilson L, Wangoo A, Silverman M, Shaw RJ. Increase in interleukin (IL)-1β and IL-6 in bronchoalveolar lavage fluid obtained from infants with chronic lung disease of prematurity. *Pediatr Res* 1996;40:250–256.
12. Tullus K, Noack G, Burman L, Nilsson R, Wretlind B, Brauner A. Elevated cytokine levels in tracheobronchial aspirate fluids from ventilator treated neonates with bronchopulmonary dysplasia. *Eur J Pediatr* 1996;155:112–116.
13. Munshi UK, Niu JO, Siddiq MM, Parton LA. Elevation of interleukin-8 and interleukin-6 precedes the influx of neutrophils in tracheal aspirates from preterm infants who develop bronchopulmonary dysplasia. *Pediatr Pulmonol* 1997;24:331–336.
14. Baier RJ, Majid A, Parupia H, Loggins J, Kruger TE. CC chemokine concentrations increase in respiratory distress syndrome and correlate with development of bronchopulmonary dysplasia. *Pediatr Pulmonol* 2004;37:137–148.
15. Dinarello CA. Biologic basis for interleukin-1 in disease. *Blood* 1996;87:2095–2147.
16. Romero R, Mazor M, Brandt F, Sepulveda W, Avila C, Cotton DB, Dinarello CA. Interleukin-1α and interleukin-1β in preterm and term human parturition. *Am J Reprod Immunol* 1992;27:117–123.
17. Yoon BH, Romero R, Jun JK, Park KH, Park JD, Ghezzi F, Kim BI. Amniotic fluid cytokines (interleukin-6, tumor necrosis factor–α, interleukin-1β, and interleukin-8) and the risk for the development of bronchopulmonary dysplasia. *Am J Obstet Gynecol* 1997;177:825–830.
18. Bry K, Whitsett JA, Lappalainen U. IL-1β disrupts postnatal lung morphogenesis in the mouse. *Am J Respir Cell Mol Biol* 2007;36:32–42.
19. Maeda Y, Dave V, Whitsett JA. Transcriptional control of lung morphogenesis. *Physiol Rev* 2007;87:219–244.
20. Breuss JM, Gillet N, Lu L, Sheppard D, Pytela R. Restricted distribution of integrin β6 mRNA in primate epithelial tissues. *J Histochem Cytochem* 1993;41:1521–1527.
21. Breuss JM, Gallo J, DeLisser HM, Klimanskaya IV, Folkesson HG, Pittet JF, Nishimura SL, Aldape K, Landers DV, Carpenter W. Expression of the β6 integrin subunit in development, neoplasia and tissue repair suggests a role in epithelial remodeling. *J Cell Sci* 1995;108:2241–2251.
22. Huang XZ, Wu JF, Cass D, Erle DJ, Corry D, Young SG, Farese RVJ, Sheppard D. Inactivation of the integrin β6 subunit gene reveals a role of epithelial integrins in regulating inflammation in the lung and skin. *J Cell Biol* 1996;133:921–928.
23. Huang X, Wu J, Zhu W, Pytela R, Sheppard D. Expression of the human integrin β6 subunit in alveolar type II cells and bronchiolar epithelial cells reverses lung inflammation in β6 knockout mice. *Am J Respir Cell Mol Biol* 1998;19:636–642.
24. Morris DG, Huang X, Kaminski N, Wang Y, Shapiro SD, Dolganov G, Glick A, Sheppard D. Loss of integrin αvβ6-mediated TGF-β activation causes Mmp12-dependent emphysema. *Nature* 2003;422:169–173.
25. Munger JS, Huang X, Kawakatsu H, Griffiths MJ, Dalton SL, Wu J, Pittet JF, Kaminski N, Garat C, Matthay MA, et al. The integrin αvβ6 binds and activates latent TGFβ1: a mechanism for regulating pulmonary inflammation and fibrosis. *Cell* 1999;96:319–328.

26. Pittet J-F, Griffiths MJD, Geiser T, Kaminski N, Dalton SL, Huang X, Brown LAS, Gotwals PJ, Koteliansky VE, Matthay MA, *et al.* TGF-β is a critical mediator of acute lung injury. *J Clin Invest* 2001;107:1537–1544.

27. Ganter MT, Roux J, Miyazawa B, Howard M, Frank JA, Su G, Sheppard D, Violette SM, Weinreb PH, Horan GS, *et al.* Interleukin-1β causes acute lung injury via αvβ5 and αvβ6 integrin–dependent mechanisms. *Circ Res* 2008;102:804–812.

28. Vicencio AG, Lee CG, Cho SJ, Eickelberg O, Chuu Y, Haddad GG, Elias JA. Conditional overexpression of bioactive transforming growth factor-β1 in neonatal mouse lung: a new model for bronchopulmonary dysplasia? *Am J Respir Cell Mol Biol* 2004;31:650–656.

29. Lappalainen U, Whitsett JA, Wert SE, Tichelaar JW, Bry K. Interleukin-1β causes pulmonary inflammation, emphysema, and airway remodeling in the adult murine lung. *Am J Respir Cell Mol Biol* 2005;32:311–318.

30. Sisson TH, Hansen JM, Shah M, Hanson KE, Du M, Ling T, Simon RH, Christensen PJ. Expression of the reverse tetracycline-transactivator gene causes emphysema-like changes in mice. *Am J Respir Cell Mol Biol* 2006;34:552–560.

31. Lukkarinen HP, Laine J, Kääpä PO. Lung epithelial cells undergo apoptosis in neonatal respiratory distress syndrome. *Pediatr Res* 2003;53:254–259.

32. Scholzen T, Gerdes J. The Ki-67 protein: from the known and the unknown. *J Cell Physiol* 2000;182:311–322.

33. Burri PH. Structural aspects of postnatal lung development: alveolar formation and growth. *Biol Neonate* 2006;89:313–322.

34. Webb DC, McKenzie ANJ, Foster PS. Expression of the Ym2 lectin-binding protein is dependent on interleukin (IL)-4 and IL-13 signal transduction: identification of a novel allergy-associated protein. *J Biol Chem* 2001;276:41969–41976.

35. Iwashita H, Morita S, Sagiya Y, Nakanishi A. Role of eosinophil chemotactic factor by T lymphocytes on airway hyperresponsiveness in a murine model of allergic asthma. *Am J Respir Cell Mol Biol* 2006;35:103–109.

36. Das KC, Ravi D. Altered expression of cyclins and CDKs in premature infant baboon model of bronchopulmonary dysplasia. *Antioxid Redox Signal* 2004;6:117–127.

37. Bland RD, Ertsey R, Mokres LM, Xu L, Jacobson BE, Jiang S, Alvira CM, Rabinovitch M, Shinwell ES, Dixit A. Mechanical ventilation uncouples synthesis and assembly of elastin and increases apoptosis in lungs of newborn mice: prelude to defective alveolar septation during lung development? *Am J Physiol Lung Cell Mol Physiol* 2008;294:L3–L14.

38. May M, Strobel P, Preisshofen T, Seidenspinner S, Marx A, Speer CP. Apoptosis and proliferation in lungs of ventilated and oxygen-treated preterm infants. *Eur Respir J* 2004;23:113–121.

39. Luyet C, Burri PH, Schittny JC. Pre- and postnatal lung development, maturation, and plasticity: suppression of cell proliferation and programmed cell death by dexamethasone during postnatal lung development. *Am J Physiol Lung Cell Mol Physiol* 2002;282:L477–L483.

40. Mao Q, Gundavarapu S, Patel C, Tsai A, Luks FI, De Paepe ME. The Fas system confers protection against alveolar disruption in hyperoxia-exposed newborn mice. *Am J Respir Cell Mol Biol* 2008;39:717–729.

41. Bhatt AJ, Pryhuber GS, Huyck H, Watkins RH, Metlay LA, Maniscalco WM. Disrupted pulmonary vasculature and decreased vascular endothelial growth factor, Flt-1, and TIE-2 in human infants dying with bronchopulmonary dysplasia. *Am J Respir Crit Care Med* 2001;164:1971–1980.

42. Frevert CW, Huang S, Danaee H, Paulauskis JD, Kobzik L. Functional characterization of the rat chemokine KC and its importance in neutrophil recruitment in a rat model of pulmonary inflammation. *J Immunol* 1995;154:335–344.

43. Schmal H, Shanley TP, Jones ML, Friedl HP, Ward PA. Role for macrophage inflammatory protein–2 in lipopolysaccharide-induced lung injury in rats. *J Immunol* 1996;156:1963–1972.

44. Kaminski N, Allard JD, Pittet JF, Zuo F, Griffiths MJD, Morris D, Huang X, Sheppard D, Heller RA. Global analysis of gene expression in pulmonary fibrosis reveals distinct programs regulating lung inflammation and fibrosis. *Proc Natl Acad Sci USA* 2000;97:1778–1783.

45. Liang TS, Wang J-M, Murphy PM, Gao J-L. Serum amyloid A is a chemotactic agonist at FPR2, a low-affinity N-formylpeptide receptor on mouse neutrophils. *Biochem Biophys Res Commun* 2000;270:331–335.

46. Raquil M-A, Anceriz N, Rouleau P, Tessier PA. Blockade of antimicrobial proteins S100A8 and S100A9 inhibits phagocyte migration to the alveoli in streptococcal pneumonia. *J Immunol* 2008;180:3366–3374.

47. Viemann D, Strey A, Janning A, Jurk K, Klimmek K, Vogl T, Hirono K, Ichida F, Foell D, Kehrel B, *et al.* Myeloid-related proteins 8 and 14 induce a specific inflammatory response in human microvascular endothelial cells. *Blood* 2005;105:2955–2962.

48. Denhardt D, Noda M, O'Regan AW, Pavlin D, Berman JS. Osteopontin as a means to cope with enviromental insults: regulation of inflammation, tissue remodeling, and cell survival. *J Clin Invest* 2001;107:1055–1061.

49. Xanthou G, Alissafi T, Semitekolou M, Simoes DCM, Economidou E, Gaga M, Lambrecht BN, Lloyd CM, Panoutsakopoulou V. Osteopontin has a crucial role in allergic airway disease through regulation of dendritic cell subsets. *Nat Med* 2007;13:570–578.

50. O'Regan A. The role of osteopontin in lung disease. *Cytokine Growth Factor Rev* 2003;14:479–488.

51. Reyburn B, Li M, Metcalfe DB, Kroll NJ, Alvord J, Wint A, Dahl MJ, Sun J, Dong L, Wang Z-M, *et al.* Nasal ventilation alters mesenchymal cell turnover and improves alveolarization in preterm lambs. *Am J Respir Crit Care Med* 2008;178:407–418.

52. Ludlow A, Yee KO, Lipman R, Bronson R, Weinreb P, Huang X, Sheppard D, Lawler J. Characterization of integrin β6 and thrombospondin-1 double-null mice. *J Cell Mol Med* 2005;9:421–437.

53. Ambalavanan N, Nicola T, Hagood J, Bulger A, Serra R, Murphy-Ullrich J, Oparil S, Chen Y-F. Transforming growth factor–β signaling mediates hypoxia-induced pulmonary arterial remodeling and inhibition of alveolar development in newborn mouse lung. *Am J Physiol Lung Cell Mol Physiol* 2008;295:L86–L95.

54. Nakanishi H, Sugiura T, Streisand JB, Lonning SM, Roberts JDJ. TGF-β–neutralizing antibodies improve pulmonary alveologenesis and vasculogenesis in the injured newborn lung. *Am J Physiol Lung Cell Mol Physiol* 2007;293:L151–L161.